Medium Range Structure of Hydrogenated Amorphous $Ti_{84}Si_{16}$

A. Pojtinger, P. Lamparter, and S. Steeb
Max-Planck-Institut für Metallforschung, Seestrasse 92, D-70174 Stuttgart
Reprint requests to Dr. P. L.; Fax: +49 711 2095420.

Z. Naturforsch. **54 a,** 704–710 (1999); received November 2, 1999

Amorphous melt-spun $Ti_{84}Si_{16}$ was investigated by small angle neutron scattering (SANS) in the blank state as well as after loading with hydrogen or deuterium. The integrated intensity and the fractal dimension of the SANS signal change strongly with increasing H, D content. A model is proposed which explains the changes of the scattering signal. By means of this model it is concluded that melt-spun amorphous $Ti_{84}Si_{16}$ consists of two types of regions. The first type contains pure Ti and the composition of the second type is $Ti_{80}Si_{20}$. The inner surfaces between these types of regions have fractal features.

Key words: Amorphous $Ti_{84}Si_{16}$; Small Angle Neutron Scattering; Hydrogen Loading.

1. Introduction

The short range order of amorphous titanium-silicides, produced by sputtering or melt-spinning, has been investigated in recent years [1, 2]. The medium range order of many amorphous alloys is characterized by inhomogeneities which give rise to a small angle neutron scattering (SANS) signal. Former investigations of hydrogenated Ti-containing amorphous alloys [3] showed that concentration fluctuations in the bulk are responsible for the SANS signal. These fluctuations may extend from some ten up to several thousand Ångstroms.

In the present work amorphous $Ti_{84}Si_{16}$ alloys which were loaded with different amounts of hydrogen were investigated by small angle neutron scattering. The hydrogen is incorporated inhomogeneously into the samples because of the inhomogeneous medium range structure of the amorphous alloy. Thus the hydrogen changes the SANS signal and can be employed as a probe for the nature of the heterogeneities. Isotopic substitution of hydrogen by deuterium causes different changes of the SANS signal owing to the opposite signs and different absolute values of the coherent scattering lengths of H and D (Table 1). In the present work a model for the composition of the inhomogeneities and the character of the inner surfaces between two types of regions is proposed which is compatible with the SANS experiments. The present model is a refinement of a model which has been proposed in a previous study [3].

Table 1. Coherent scattering lengths b [4].

	Ti	Si	H	D
b $[10^{-12}\mathrm{cm}]$	–3.438	0.4169	–0.3741	0.6674

2. Theoretical

2.1. *Differential Cross Section*

Samples which consist of two phases with different scattering length densities give rise to a SANS signal. For an isotropic system the differential cross section for coherent scattering per atom is [5, 6]

$$\frac{\mathrm{d}\sigma}{\mathrm{d}\Omega}(Q) = \frac{1}{\rho_0}\nu_1\nu_2(\Delta\eta)^2 4\pi \int R^2\gamma(R)\frac{\sin QR}{QR}\mathrm{d}R, \quad (1)$$

where $Q = 4\pi(\sin\theta)/\lambda$, 2θ = scattering angle, λ = wavelength, ρ_0 = number density of the sample, R = coordinate in real space, $\Delta\eta$ = difference of the scattering length densities of the two phases, ν_1, ν_2 = volume fractions of the two phases, $\gamma(R)$ = autocorrelation function of the scattering length density.

2.2. *Fractal Dimension*

For the SANS of metallic glasses at small Q-values often a power-law $I(Q) \sim Q^{-S}$ was observed, where

0932–0784 / 99 / 1200–0704 $ 06.00 © Verlag der Zeitschrift für Naturforschung, Tübingen · www.znaturforsch.com

Dieses Werk wurde im Jahr 2013 vom Verlag Zeitschrift für Naturforschung in Zusammenarbeit mit der Max-Planck-Gesellschaft zur Förderung der Wissenschaften e.V. digitalisiert und unter folgender Lizenz veröffentlicht: Creative Commons Namensnennung-Keine Bearbeitung 3.0 Deutschland Lizenz.

Zum 01.01.2015 ist eine Anpassung der Lizenzbedingungen (Entfall der Creative Commons Lizenzbedingung „Keine Bearbeitung“) beabsichtigt, um eine Nachnutzung auch im Rahmen zukünftiger wissenschaftlicher Nutzungsformen zu ermöglichen.

This work has been digitalized and published in 2013 by Verlag Zeitschrift für Naturforschung in cooperation with the Max Planck Society for the Advancement of Science under a Creative Commons Attribution-NoDerivs 3.0 Germany License.

On 01.01.2015 it is planned to change the License Conditions (the removal of the Creative Commons License condition “no derivative works”). This is to allow reuse in the area of future scientific usage.

Table 2. Blank and hydrogenated $Ti_{84}Si_{16}$; $c_{H(D)}$: H, D content [at-%], $f_{H(D)}$: enhancement factor of SANS according to (3), D_S: fractal dimension.

Series of experiments	$c_{H(D)}$	$\sqrt{f_{H(D)}}$	D_S
I	0 (H)		2.76
	10 (H)	2.1	2.78
	12 (H)	2.1	2.69
	34 (H)	2.3	2.60
	41 (H)	4.9	2.25
	0 (D)		2.85
	3 (D)	1.4	2.71
	6 (D)	1.2	2.81
	16 (D)	1.5	2.77
	19 (D)	1.4	2.69
II	0 (H)		2.68
	24 (H)	2.0	2.59
	26 (H)	1.4	2.78
	36 (H)	1.8	2.70
	51 (H)	1.6	2.55
	0 (D)		2.73
	13 (D)	1.4	2.86
	15 (D)	1.6	2.70
	20 (D)	1.4	2.72
	31 (D)	1.4	2.78
III	0 (H)		2.68
	45 (H)	3.5	2.33
	0 (D)		2.73
	30 (D)	1.9	2.62

$-S$ was found in the range between −3 and −4. According to [7] it is possible to introduce a fractal dimension D_S of the surface of the scattering regions:

$$I(Q) \sim Q^{-6+D_S} = Q^{-S}. \qquad (2)$$

For $D_S = 2$ the surface is smooth and for $D_S > 2$ the surface has fractal properties which means that it is rough. The power-law scattering of amorphous metals with $-4 \le -S \le -3$ can be explained by the existence of inner self-similar surfaces whose roughness is characterized by a fractal dimension $2 \le D_S \le 3$.

2.3. *Enhancement Factor*

To compare the strength of the SANS signal of the H(D) loaded samples, $I_{H(D)}(Q)$, with that of an unloaded sample, $I_0(Q)$, an enhancement factor $f_{H(D)}$ is defined:

$$\int I_{H(D)}(Q)\mathrm{d}Q = f_{H(D)} \int I_0(Q)\mathrm{d}Q. \qquad (3)$$

3. Experimental

3.1. *Specimen Preparation*

Amorphous $Ti_{84}Si_{16}$ ribbons were produced by the melt-spinning method [8]. The ribbons were several meters long, between one and two millimeters wide and 20 to 30 μm thick. The H(D) loading was done by electrolysis. The ribbons were wound around a cylindrical PVC frame and were connected with a Cu-cathode. In the center of the PVC frame a Pd wire was fixed as an anode. A 1 M solution of H_2SO_4 (D_2SO_4) was used as electrolyte. The temperature of the electrolyte was 65 °C, the current 50 mA and the voltage 2.4 V. The process of H(D) loading for the higher H(D) contents took several hours. An undesired effect was the thickness reduction of the ribbons by etching. Thus the final thickness of the higher loaded ribbons was only between 10 and 15 μm. The time needed for the D loading was about twice as long as for the H loading. Therefore it was not possible to prepare samples with more than 31 at-% D. In Table 2 the H(D) loaded samples are listed. After the loading process the H(D) content of the samples was analyzed by the method of carrier-gas hot-extraction at 1100 °C. X-ray diffraction showed that the samples were still amorphous after H(D) loading. For the SANS experiments it was necessary to fix up to 50 layers of ribbons on top of each other.

3.2. *Small Angle Scattering*

The SANS experiments were performed at Laboratoire Léon Brillouin, CEA-CNRS, C.E. Saclay, France with the instrument PACE and at Hahn Meitner Institut, Berlin, Germany with the instrument V4. At PACE two different settings (λ = 6 Å, sample-detector distance SD = 2.5 m and λ = 14 Å, SD = 4.7 m) were chosen to cover by overlapping runs the Q-range from $2.8 \cdot 10^{-3}$ Å^{-1} up to 0.13 Å^{-1}. At V4 three different settings (SD = 1m, 4m, 16m, λ = 14 Å for all three settings) were needed to cover the Q-range from $3.8 \cdot 10^{-3}$ Å^{-1} up to 0.27 Å^{-1}. For the experiments at PACE the samples have to be isotropic, because this instrument delivers only one-dimensional data. The isotropic scattering of the samples was confirmed at V4 which is equipped with a two-dimensional detector.

The measured intensities were corrected for background and absorption. The conversion into absolute

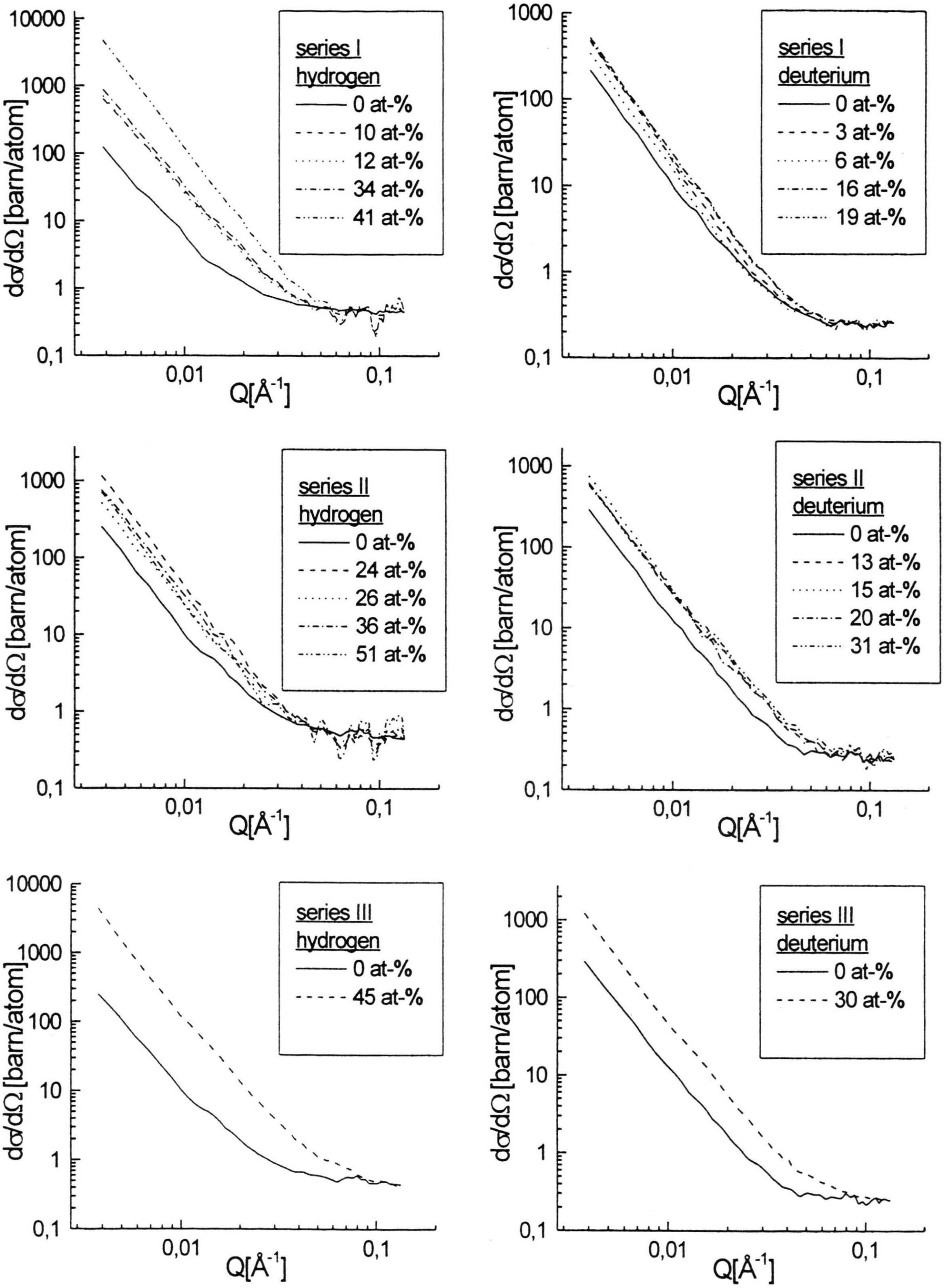

Fig. 1. Small angle neutron scattering cross sections with blank (0 at-% H) and H(D) loaded amorphous $Ti_{84}Si_{16}$: log-log plot of $d\sigma/d\Omega$ versus Q for three series of samples.

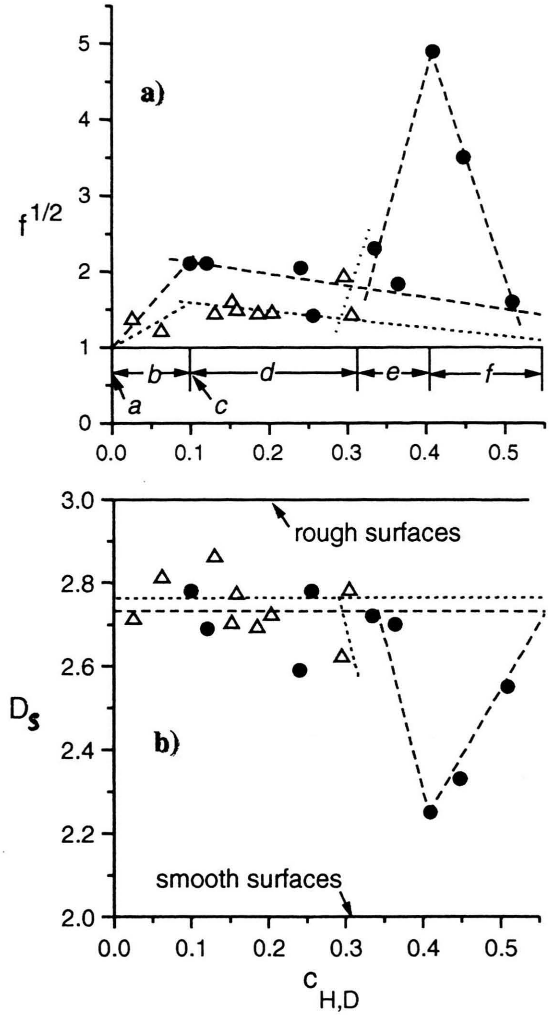

Fig. 2. a) enhancement factor $f^{1/2}$ of the SANS signal due to H(D) loading according to (3), b) fractal dimension D_S of the inner surfaces according to (2). • loaded with H, Δ loaded with D. The dashed lines (long for H, short for D) show the trends of $f^{1/2}$ and D_S versus $c_{H,D}$ as guide for the eye.

scattering units was done with the incoherent scattering signal from a vanadium standard in the range $Q > 0.1$ Å^{-1}.

4. Results

Figure 1 shows the scattering cross sections of the H(D) loaded samples and the corresponding blank samples in a log-log plot. According to [7] and (2) the fractal dimension D_S of inner self-similar surfaces was determined from the gradient of the SANS signal in a log-log plot. The enhancement factor $f_{H(D)}$ was determined as defined in (3). D_S and $f_{H(D)}$ are listed in Table 2. Figure 2a) shows the square root of $f_{H(D)}$ and Fig. 2b) the fractal dimension D_S.

The square root of the enhancement factor increases with increasing H(D) content up to about 10 at-% H(D). The value of $f_H{}^{1/2}$ is twice as high as $f_D{}^{1/2}$. From 10 at-% to 30 at-% H(D), $f_H{}^{1/2}$ and $f_D{}^{1/2}$ decrease with increasing H(D) content. But then the SANS signal increases very strongly for concentrations up to 41 at-% H, whereas D_S becomes smaller. For H contents higher than 41 at-% the SANS signal decreases and D_S increases. This rather surprising result will be explained in the following section by means of a model.

5. Discussion

A SANS signal can be produced by an inhomogeneous distribution of the scattering length density inside the irradiated volume. This may be caused by density fluctuations or by compositional fluctuations [3]. On the other side, also irregularities on the outer surfaces of the amorphous ribbons have to be considered as a possible source of SANS [9]. However, ribbons with different thicknesses, i. e. with different ratios of the outer surface to their volume were measured and no correlation between the SANS signal and the relative amount of outer surfaces was observed. Therefore, in the case of the $Ti_{84}Si_{16}$ ribbons investigated in the present work, the SANS had to be attributed to the volume. The possible sources of the SANS signal were investigated in [3], and the result for melt-spun $Ni_{16}Ti_{68}Si_{16}$ was that the SANS signal cannot be caused by fluctuations of the local atomic number density alone but must be due to compositional fluctuations. Of course, these give rise also to density fluctuations depending on the different molar volumes of the constituents.

A further important point for the following considerations is that according to (1) the SANS signal is proportional to the product of the volume fractions of the two phases with different scattering length densities. Furthermore, the SANS signal is proportional to the square of the difference $\Delta\eta$ of the scattering length densities. Therefore the square root of $f_{H(D)}$ is plotted in Fig. 2a) as a measure of the contrast $\Delta\eta$. The dependence of $f_{H(D)}$ on the H(D) content in Fig. 2a) does not show a monotonous behaviour but indicates

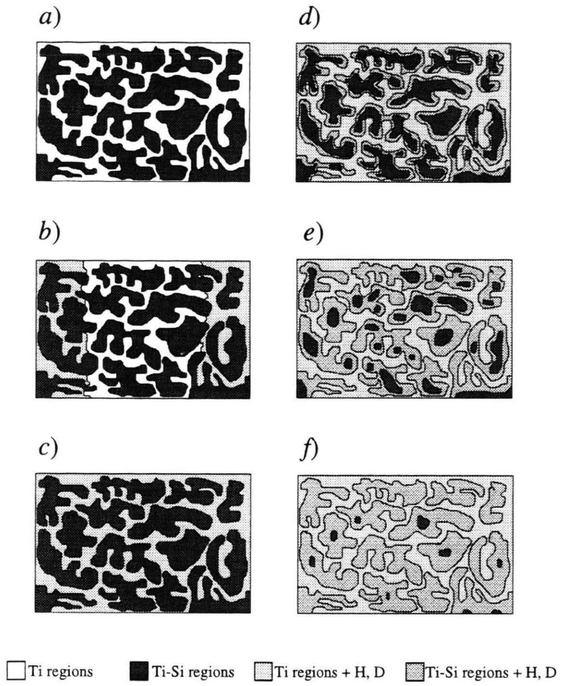

Fig. 3. Model for the process of H(D) loading of amorphous $Ti_{84}Si_{16}$ with increasing H(D) content at different stages. a) without H(D), b) diffusion of H(D) into Ti regions, c) Ti regions saturated with H(D), d-f) diffusion of H(D) into Ti-Si regions. At stage f) the Ti-Si regions are almost saturated.

a quite complicated nature of the H(D) incorporation, where three rather surprising effects occur:

1) The scattering lengths of H and D have opposite signs. Thus one would expect that an increase of the SANS signal due to H loading would be accompanied by a decrease of the SANS signal due to D loading, and vice versa. However, the SANS signal for the H loaded samples as well as for the D loaded samples is higher than for the blank samples.

2) The absolute value of the scattering length of D is about twice as large as that of H. According to (3) we would expect the ratio of $f_H{}^{1/2}/f_D{}^{1/2}$ to be about 0.5. However, Fig. 2a) shows that the ratio is about 2.

3) The third remarkable effect is the strong increase of $f_H{}^{1/2}$ in the range from 30 at-% H to 41 at-% H. This increase is accompanied by a decrease of the fractal dimension D_S in Figure 2b).

In the following a model for the explanation of these effects is proposed which is illustrated by means of the Figures 2 - 4. The model is based on the view that in Ti rich amorphous ribbons, such as $Ti_{84}Si_{16}$, there are regions (I) consisting of Ti only, and regions (II) which contain Ti and Si. The H(D) concentration range in Fig. 2a) can be subdivided into the ranges a-f where apparently different structural phenomena occur which will be discussed in the following.

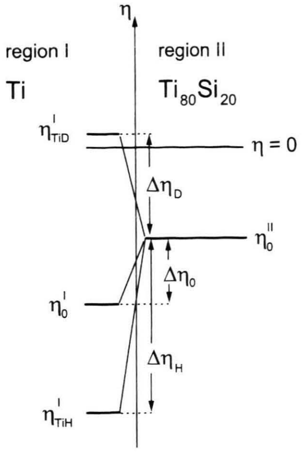

Fig. 4. Sketch of the scattering length densities η and differences $\Delta\eta$ for the two types of regions, Ti and $Ti_{80}Si_{20}$. η_0: without H(D), $\eta_{TiH(D)}$: with H(D).

Ranges a, b, c

Wide angle scattering with hydrogenated $Ti_{84}Si_{16}$ [10] showed that the hydrogen atoms prefer Ti nearest neighbours. Thus it can be assumed that H(D) atoms first of all occupy the Ti regions. This behaviour is illustrated in Figs. 3a), b), c) and corresponds to the ranges a, b, c in Figure 2a). The scattering length density of the pure Ti regions is more negative than that of the Ti-Si regions because the scattering length of Ti is negative and that of Si is positive. Note, that for the Ti-Si regions the scattering length density is negative, too, because of the higher Ti content. Figure 4 illustrates this case. $\eta_0{}^{I}$ is the scattering length density for the blank Ti regions and $\eta_0{}^{II}$ for the blank Ti-Si regions. $\Delta\eta_0$ is the difference of the scattering length densities in the blank samples. It is clear that H in region I increases the contrast $\Delta\eta_H$, whereas D first causes a decrease up to a D content where $\eta_{TiD}{}^{I} = \eta_0{}^{II}$. Then the contrast increases again with increasing D content. This would mean, that the SANS signal of the D loaded samples has to decrease until $\eta_{TiD}{}^{I} = \eta_0{}^{II}$. At this point no SANS signal should be visible. With further addition of D the SANS signal must increase again. However this behaviour was not observed. The SANS signal of the D loaded sample is always higher than for the blank sample. This behaviour can be explained by the idea that the D atoms permeate the regions I as a diffusion front (Fig. 3b)). In the part of the loaded Ti regions the D content is always higher than the D content for $\eta_{TiD}{}^{I} = \eta_{0}{}^{II}$. This case is shown in Fig. 4, where $\eta_{TiD}{}^{I} > \eta_{0}{}^{II}$. $\Delta\eta_{H(D)}$ is the difference of the scattering length densities between the H(D) loaded part of regions I and the unloaded regions II. The H and D atoms form a diffusion front which has permeated the Ti regions completely in Figure 3c). When the Ti regions are permeated completely, the difference of the scattering length densities will have a maximum. This maximum can be determined at 10 at-% H(D) in Fig. 2a), point c. Note, that the H(D) content in the regions I is about 36 at-% because the value of 10 at-% refers to the whole sample (see below).

Now it is possible to make a statement about the composition of the two types of regions. The supposition is that regions I consist of titanium only and that these regions are completely permeated at 10 at-% H(D). Then the Ti content of regions II can be determined from the condition that the calculated values of $f_{H}{}^{1/2}$ and $f_{D}{}^{1/2}$ correspond to the experimental values. The difference of the scattering length densities for the blank sample can be calculated from

$$|\eta^{I}_{Ti} - \eta^{II}_{TiSi}| = |\rho^{I}_{Ti} b_{Ti} - \rho^{II}_{TiSi}(c^{II}_{Ti} b_{Ti} + c^{II}_{Si} b_{Si})|, \quad (4)$$

where ρ denotes number densities, and $c^{II}_{Ti} + c^{II}_{Si} = 1$.

The difference of the scattering length densities for the H(D) loaded sample, where H(D) is embedded only in regions I, is:

$$|\eta^{I}_{TiH(D)} - \eta^{II}_{TiSi}| = |\rho^{I}_{TiH(D)}(c^{I}_{Ti} b_{Ti} + c^{I}_{H(D)} b_{H(D)}) - \rho^{II}_{TiSi}(c^{II}_{Ti} b_{Ti} + c^{II}_{Si} b_{Si})|, \quad (5)$$

where $c^{I}_{Ti} + c^{I}_{H(D)} = 1$ and $c^{II}_{Ti} + c^{II}_{Si} = 1$.

The volume fractions of both types of regions are constant, and thus it is not necessary to take them into account. Now we obtain the following result: If there is an amount of 10 at-% H(D) in the $Ti_{84}Si_{16}$ alloy, corresponding to the first maximum of $f_{H(D)}{}^{1/2}(c_{H(D)})$, and if this amount is incorporated only in the Ti regions I, the value of $f_{H}{}^{1/2}$ will be 2.3 and the value of $f_{D}{}^{1/2}$ will be 1.4, in case the composition of the regions II is $Ti_{80}Si_{20}$. These values of $f_{H}{}^{1/2}$ and $f_{D}{}^{1/2}$ agree with the experimental results in Figure 2a). That means that the amorphous $Ti_{84}Si_{16}$ alloy is phase separated into Ti regions and $Ti_{80}Si_{20}$ regions. The H(D) content in the Ti region is 36 at-%.

Ranges d, e, f

When the regions I are permeated completely, further H(D) will begin to be incorporated also in regions II (Fig. 3d)). This will reduce the contrast between the regions I and II and thus cause a decrease of $f_{H(D)}{}^{1/2}$. This behaviour can be observed in Fig. 2a) up to about 30 at-% H(D).

In the range e from about 30 at-% H to 41 at-% H the SANS signal increases very strongly. At the same time, the fractal dimension D_{S}, which is ascribed to the inner surfaces, decreases. This means that within this H(D) composition range there are new and smoother inner surfaces which separate two areas with different scattering length density. This effect can be observed with the D loaded samples, too, but only allusively because samples with more than 31 at-% D could not be prepared by electrolysis. The H inside the samples must be responsible for this smoother inner surfaces, assuming that the structure of the samples is not changed by the H loading. This effect must be dominant because $f_{H}{}^{1/2}$ increases strongly. At 41 at-% H, $f_{H}{}^{1/2}$ starts to decrease and the fractal dimension D_{S} increases.

These experimental results can be incorporated into the model. Figures 3d), e), f) illustrate the process of the diffusion of the H atoms inside the $Ti_{84}Si_{16}$ ribbons. Figure 3d) shows the beginning of the diffusion of H into the regions II, which causes a reduction of the difference of the scattering length densities between regions I and II. But with increasing H content in regions II a new diffusion front is built up, which leads to a new difference of the scattering length densities and an additional contribution to the SANS signal. At the beginning of the diffusion of H through the fractal inner surfaces the change of the fractal dimension D_{S} is very small (range d). Figures 3d) and e) illustrate why D_{S} becomes smaller with increasing H content in the regions II (range e). The areas near the fractal inner surfaces are loaded with H gradually, and thus H permeates the regions II in form of a smoother diffusion front and D_{S} becomes smaller. For the dominance of this effect there are two reasons.

Firstly the contrast between regions I and regions II becomes smaller, and secondly the regions II occupy about 80% of the volume of the whole sample. The SANS signal which is caused by the diffusion front of H in the regions II is proportional to the product of the loaded and the unloaded volumes of the regions II. At the beginning of H diffusion into the regions II the product of the loaded and unloaded volumes of the regions II is very small and the surface of the diffusion front is very rough. Are the volumes of the loaded and the unloaded parts of the regions II the same, their product attains the maximum value and thus the SANS from the regions II will be maximum (around $c_H = 0.4$ in Fig. 2a)). The diffusion front is very smooth and this effect dominates ($D_S = 2.2$ in Fig. 2b)). With increasing H content of the regions II the product of the loaded and unloaded volume fractions and thus the dominance of this effect again decreases. D_S becomes larger, because the SANS effect between regions I and II will be less covered by the effect of the diffusion front in regions II. When the regions II are permeated completely by H, only the contrast between regions I and II remains, but now its level is lower because the contrast is reduced due to the fully loaded regions II.

6. Conclusions

Amorphous melt-spun $Ti_{84}Si_{16}$ exhibits a small angle neutron scattering (SANS) effect, which is caused by compositional fluctuations. The SANS signal is changed by loading the $Ti_{84}Si_{16}$ ribbons with hydrogen or deuterium. On the basis of these changes a model of H(D) diffusion into amorphous $Ti_{84}Si_{16}$ alloys is introduced. It is suggested that the medium range order of the amorphous alloy consists of two types of regions, Ti and $Ti_{80}Si_{20}$. The volume fraction of the Ti regions is about 20 pct. The inner surfaces between the two types of regions have a fractal character.

Acknowledgements

We are grateful to L. Auvray, LLB Saclay and A. Wiedenmann and U. Keiderling, HMI Berlin, for help during the SANS experiments. We would also like to thank Laboratoire Léon Brillouin and Hahn Meitner Institut for allocation of beam time. This work was supported by the Deutsche Forschungsgemeinschaft through grant La 686/2 and by the Human Capital and Mobility Program of the European Community.

[1] A. Pojtinger, R. Bellissent, P. Lamparter, and S. Steeb, Z. Naturforsch. **50a**, 749 (1995).
[2] P. Lamparter, A. Habenschuss, and A. H. Narten, J. Non-Cryst. Sol. **86**, 109 (1986).
[3] P. Lamparter and B. Boucher, Z. Naturforsch. **48a**, 1086 (1993).
[4] L. Köster and E. Seyman, Atomic Data and Nuclear Data Tables **49**, 65 (1991).
[5] A. Guinier and G. Fournet, Small Angle Scattering of X-Rays, John Wiley & Sons, New York 1955.
[6] O. Glatter and O. Kratky, Small Angle X-Ray Scattering, Academic Press, New York 1982.
[7] J. E. Martin and A. J. Hurd, J. Appl. Cryst. **20**, 61 (1987).
[8] E. H. Strange and C. A. Pim, U.S. Pat. 905758. 1908.
[9] H. Träuble, P. Lamparter, and S. Steeb, J. Phys. I France **2**, 1029 (1992).
[10] P. Lamparter and S. Steeb, Physica B **180&181**, 782 (1992).